Observational Evidence for Dependencies of Cloud Properties and Radiative Fluxes by Cloud Types on Measures of the Degree of Convective Aggregation

Kuan-Man Xu[1], Yaping Zhou[2], Moguo Sun[1,3], Yongxiang Hu[1]

[1]NASA Langley Research Center, Hampton, VA; [2]UMBC/NASA Goddard Space Flight Center; [3]Science Systems and Applications, Inc.. Email: Kuan-Man.Xu@nasa.gov

1. Introduction

Convective aggregation includes a mode of self-aggregation phenomenon appearing in idealized radiative-convective equilibrium simulations under constant, uniform sea surface temperature, with humid clusters surrounded by dry patches. There is lack of observational evidence for fully supporting the modeled phenomenon. In particular, in-cloud properties are not well understood and diverse measures of the degree of convective aggregation are used in different studies. This study examines the dependencies of cloud properties and radiative fluxes by cloud types on measures of the degree of convective aggregation using observations from CERES data products combined with MERRA-2 reanalysis data.

2. Data sets and methodology

Three data sets are used in this study:

1) CERES footprint data for defining three morphology measures of aggregation (see box for detailed definitions);

✦ Simple Convective Aggregation Index (SCAI) (Tobin *et al.* 2012)

- $SCAI = \frac{N}{N_{max}}\frac{D_1}{L}\times 1000$ (SCAI > 0)
- N: number of cloud objects; L domain lengthscale
- N_{max}: maximum of cloud objects within a domain
- D_1 is the geometrical mean of distances ($d_{i,j}$) between objects; $D_1 = \sum_{i=1}^{N}\sum_{j=i+1}^{N} d_{i,j} \Big/ \frac{1}{2}N(N-1)$

✦ A modification to SCAI (MCAI)

- Reduce the distances ($d_{i,j}$) between centroids of two objects by sum of their radii
- $d'_{i,j} = d_{i,j} - (\sqrt{A_i} + \sqrt{A_j})/\sqrt{\pi}$
- $D_2 = \sum_{i=1}^{N}\sum_{j=i+1}^{N} d'_{i,j} \Big/ \frac{1}{2}N(N-1)$
- MCAI → 0 as D_2 → 0, but SCAI is always > 0 because $D_1 > 0$

✦ Convective Organization Potential (COP) (White *et al.* 2018)

- Interaction potential: $V(i,j) = \frac{\sqrt{A_i}+\sqrt{A_j}}{d(i,j)\sqrt{\pi}}$
- $COP = \sum_{i=1}^{N}\sum_{j=i+1}^{N} V(i,j) \Big/ \frac{1}{2}N(N-1)$
- A_i, A_j are areas of i^{th} and j^{th} objects, respectively
- 0 ≤ COP ≤ 1 (maximum aggregation)

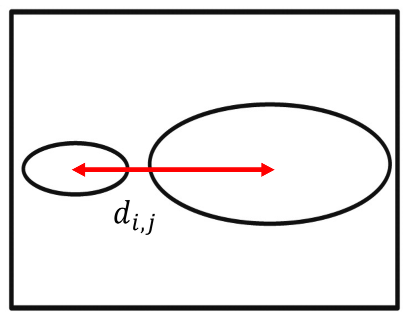

2) MERRA-2 data for calculating the thermodynamic- or dynamic-based aggregation measures: column moist static energy (CH), relative humidity (CRH), and vapor variance (PWV), column-averaged RH (ARH), subsidence fraction (SF) and ascending fractions according to omega at 500 (AF1) and column-averaged omega (AF2).

3) CERES flux-by-cloud-type (FBCT) for cloud fraction, in-cloud properties and TOA radiative fluxes categorized by effective cloud pressure (p_c) - cloud optical depth (τ) pairs.

Fig. 1. MCAI vs. SCAI, COP & MERRA-2 measures

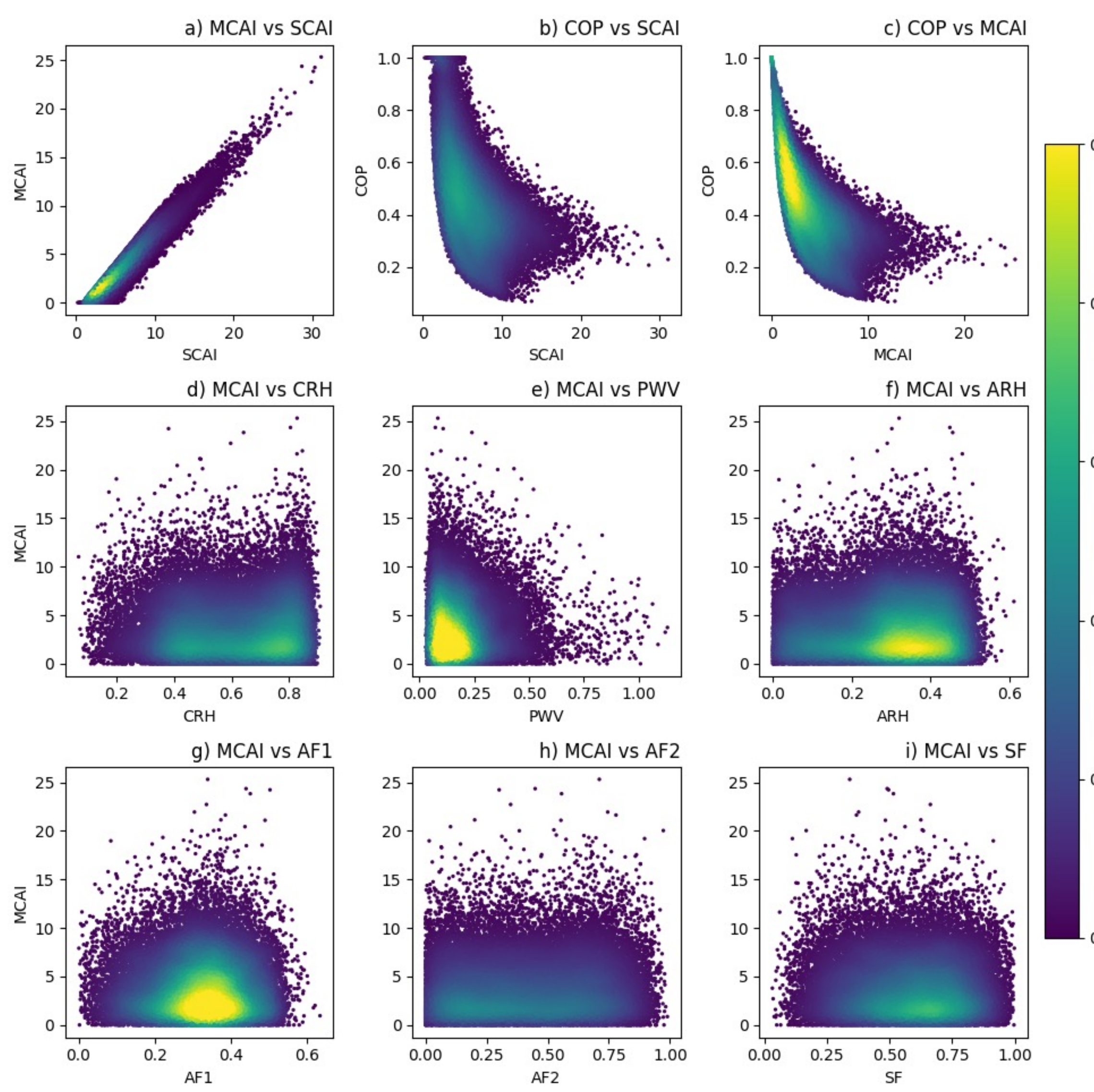

We match these measures over 10° x10° grids to the same regions in the FBCT data and divide the entire population (~30,000) into three equal-size sub-populations (i.e., low, moderate and strong aggregation) for a given measure. Cloud fraction and property and radiative flux differences between strong and weak aggregation subsets are obtained according to cloud type (Figs. 3-6). The analysis domain covers the tropical belt (25°S-25°N) for 2006-2010.

3. Results

Fig. 2. CRH vs. other MERRA-2 measures

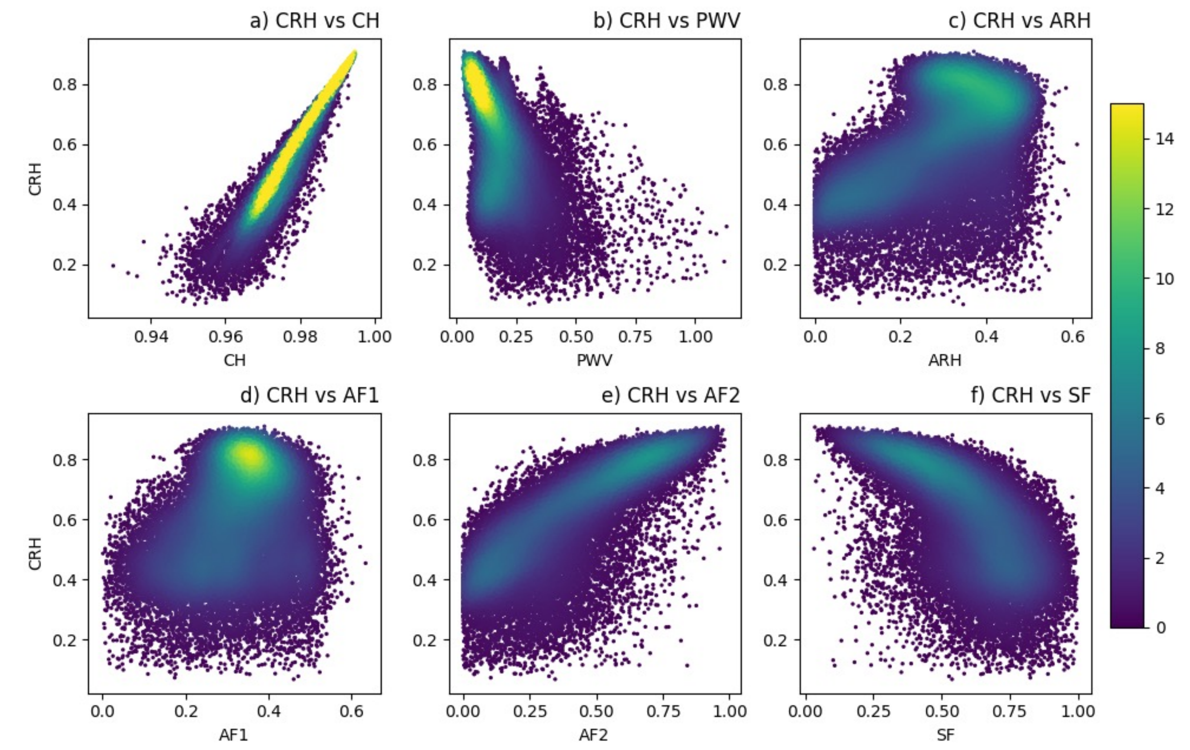

Fig. 3. Total cloud fraction by cloud type

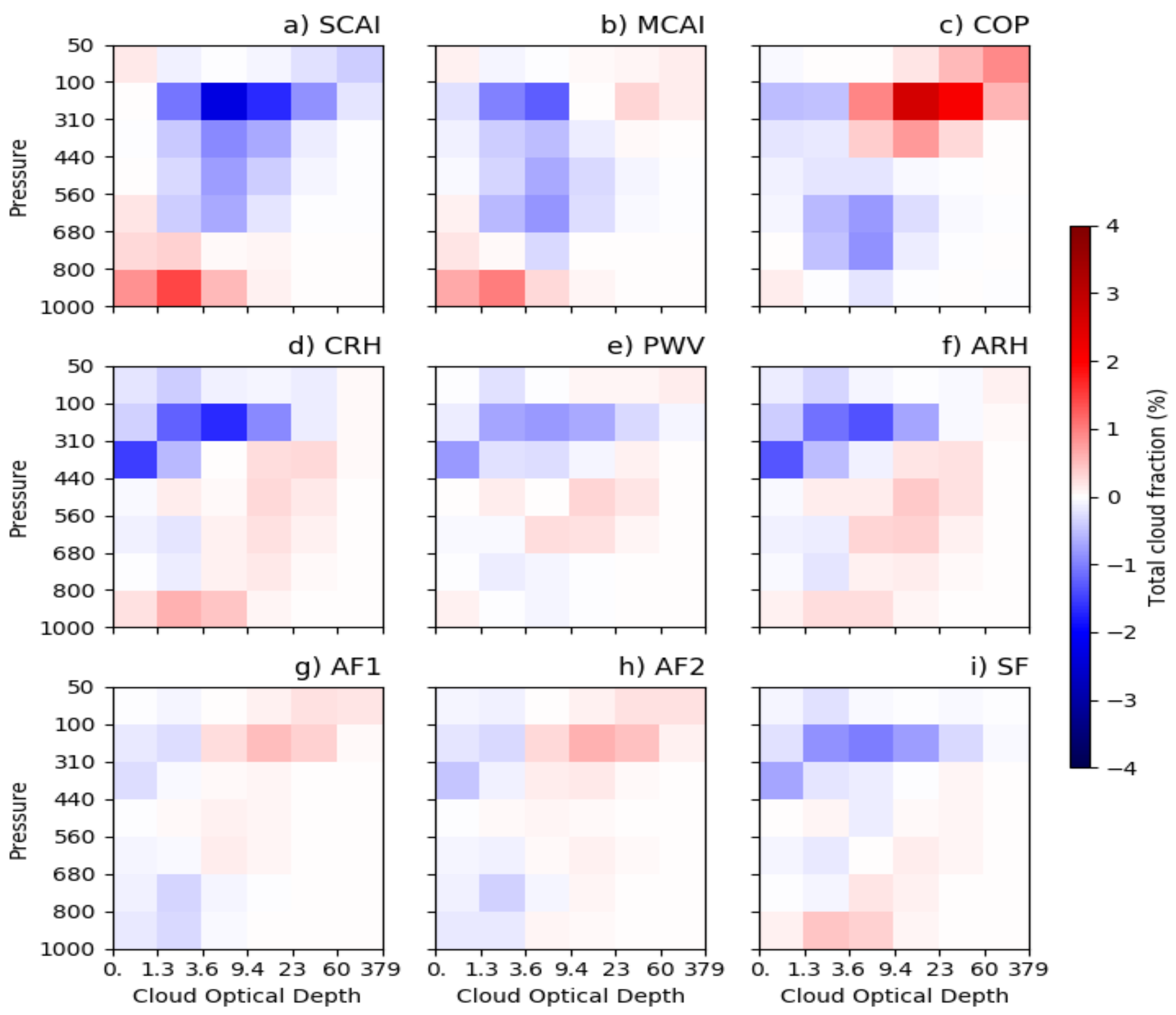

Fig. 4. Cloud optical depth by cloud type

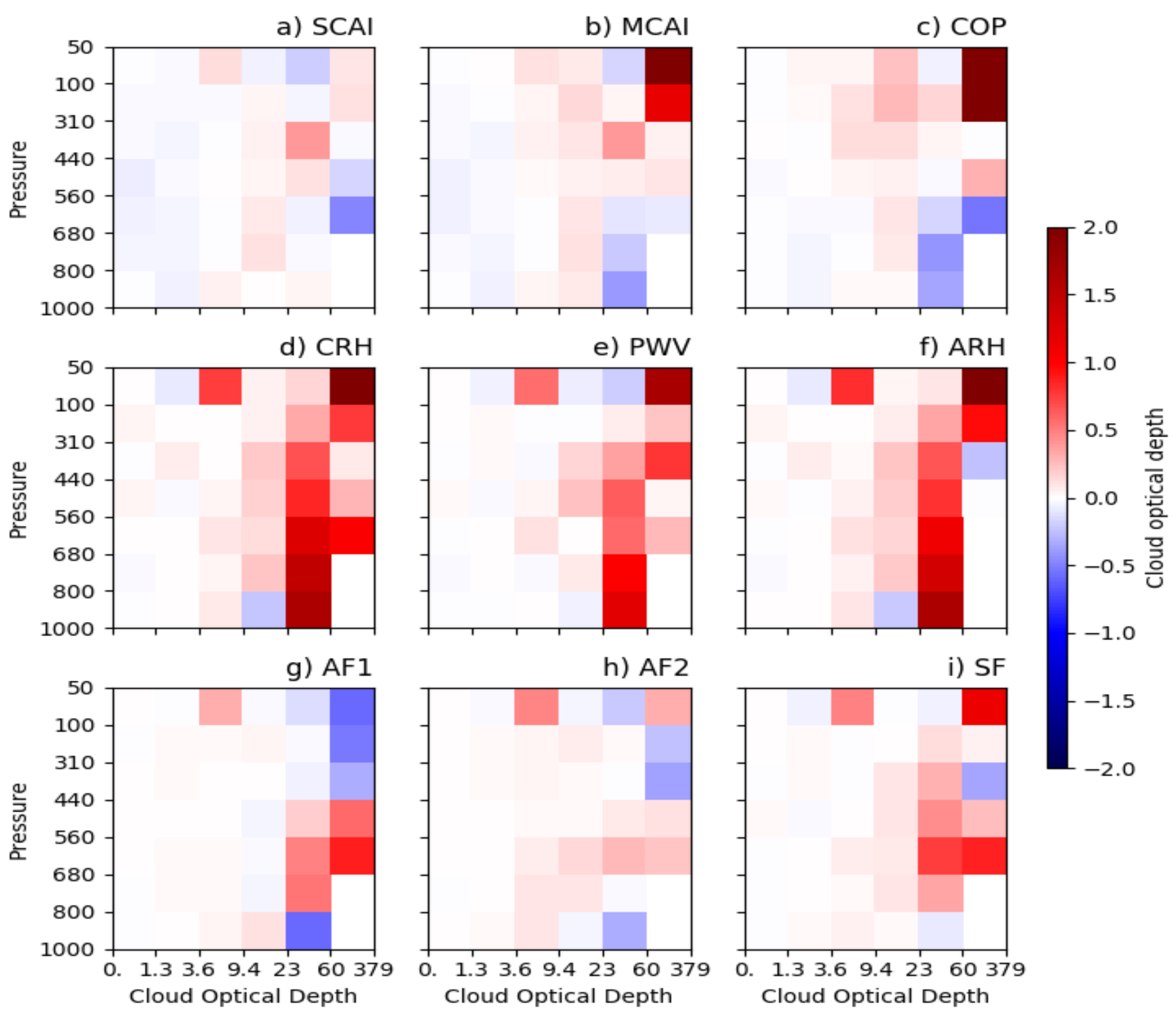

4. Summary of results

1. MCAI is more closely related to COP than SCAI is despite of the strong correlation between SCAI and MCAI (top panels of Fig. 1).
2. In general, there is not much correlation between MCAI (SCAI, COP, as well) and MERRA-2 derived dynamic and thermodynamic measures (bottom two rows of Fig. 1), MERRA-2 derived measures show more physical consistency among themselves, particularly for the weakly aggregated states (Fig. 2).
3. Relative to weak aggregation, there are less frequent occurrences of high clouds and more frequencies of low clouds for strong aggregation, except for optically thick high clouds of COP, AF1 and AF2 (Fig. 3).
4. Cloud optical depths (Fig. 4) change little from weak to strong aggregation except for some optically cloud types.
5. There are large contrasts in LW and SW differences between the morphology indices (SCAI/MCAI/COP) and MERRA-2 measures (Figs. 5 and 6). *Need to calculate SW differences from those of albedo multiplied by insolation.*
6. Different geographic locations of weak/strong aggregation populations play a key role in contributing to above results.

Fig. 5. Longwave radiative flux (LW) by cloud type

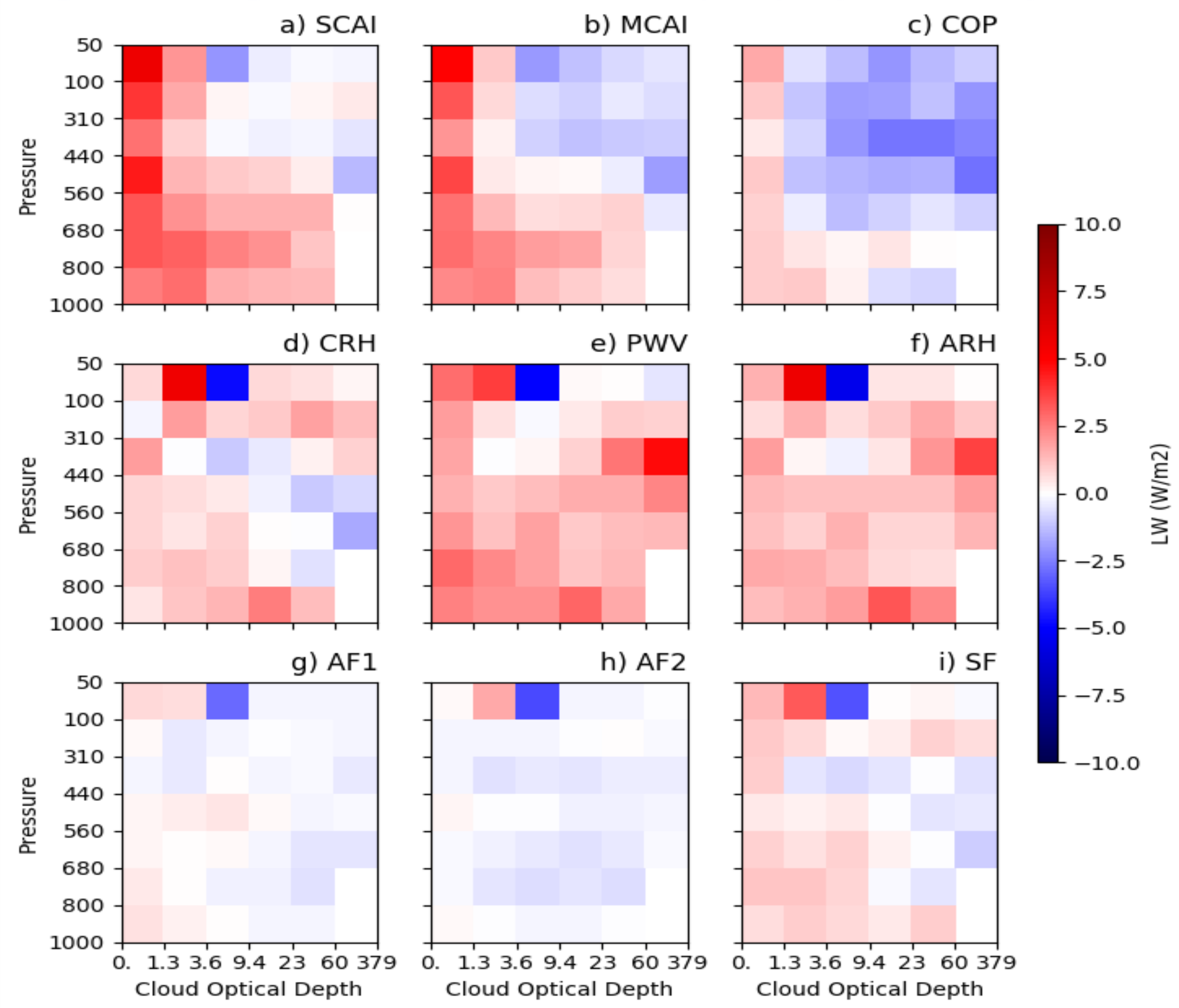

Fig. 6. Solar radiative flux (SW) by cloud type